



## A novel Apigenin derivative suppresses renal cell carcinoma via directly inhibiting wild-type and mutant MET

Jing Li<sup>a,1</sup>, Guishan Tan<sup>a,b,1</sup>, Yabo Cai<sup>c</sup>, Ruihuan Liu<sup>a,d</sup>, Xiaolin Xiong<sup>c</sup>, Baohua Gu<sup>c</sup>, Wei He<sup>c</sup>, Bing Liu<sup>c</sup>, Qingyun Ren<sup>c</sup>, Jianping Wu<sup>a</sup>, Bo Chi<sup>c</sup>, Hang Zhang<sup>c</sup>, Yanzhong Zhao<sup>e</sup>, Yangrui Xu<sup>a</sup>, Zhenxing Zou<sup>a</sup>, Fenghua Kang<sup>a</sup>, Kangping Xu<sup>a,\*</sup>

<sup>a</sup> Xiangya School of Pharmaceutical Sciences, Central South University, Changsha 410013, China

<sup>b</sup> Xiangya Hospital of Central South University, Changsha 410008, China

<sup>c</sup> State Key Laboratory of Anti-Infective Drug Development, Sunshine Lake Pharma Co. Ltd, Dongguan 523871, China

<sup>d</sup> Zhuzhou Qianjin Pharmaceutical Co. Ltd, Zhuzhou, 412007, China

<sup>e</sup> The Third Xiangya Hospital, Central South University, Changsha 410013, China

### ARTICLE INFO

#### Keywords:

Apigenin derivatives  
Renal cell carcinoma  
MET  
MET downstream signaling  
Drug-resistant MET mutations

### ABSTRACT

MET, the receptor of hepatocyte growth factor (HGF), is a driving factor in renal cell carcinoma (RCC) and also a proven drug target for cancer treatment. To improve the activity and to investigate the mechanisms of action of Apigenin (APG), novel derivatives of APG with improved properties were synthesized and their activities against Caki-1 human renal cancer cell line were evaluated. It was found that compound **15e** exhibited excellent potency against the growth of multiple RCC cell lines including Caki-1, Caki-2 and ACHN and is superior to APG and Crizotinib. Subsequent investigations demonstrated that compound **15e** can inhibit Caki-1 cell proliferation, migration and invasion. Mechanistically, **15e** directly targeted the MET kinase domain, decreased its auto-phosphorylation at Y1234/Y1235 and inhibited its kinase activity and downstream signaling. Importantly, **15e** had inhibitory activity against mutant MET V1238I and Y1248H which were resistant to approved MET inhibitors Cabozantinib, Crizotinib or Capmatinib. *In vivo* tumor graft study confirmed that **15e** repressed RCC growth through inhibition of MET activation. These results indicate that compound **15e** has the potential to be developed as a treatment for RCC, and especially against drug-resistant MET mutations.

### 1. Introduction

Renal cell carcinoma (RCC), a major form of kidney cancer, is one of the most common cancers worldwide [1]. Clear cell RCC [2] and papillary RCC [3] account for approximately 75% of RCC and 15% of all kidney cancers respectively [1]. Although nephrectomy is an effective therapy for most patients with localized disease, metastasis occurs in many patients ultimately experience disease relapse [4]. There are still tremendous unmet medical needs for RCC therapy.

In addition to inactivation of Von Hippel-Lindau disease tumor suppressor (VHL) which is a hallmark and an important driving factor

for clear cell RCC [4], receptor tyrosine kinase (RTK) MET activation is also an important factor in renal cancer progression [5]. MET, the receptor for hepatocyte growth factor (HGF), is normally activated by HGF binding but can also be activated by mutations and gene amplification and overexpression [6]. During the process of MET activation, auto-phosphorylation at Y1234 and Y1235 after MET dimerization is critical and an indicator for its kinase activity [7]. Once activated, MET transduces signals down toward RTK classical pathways including PI3K-Akt, Ras-Raf-MEK-Erk and Stat3 to regulate cell survival, growth, proliferation, and mobility [8]. In RCC, MET is activated by mutation and upregulated expression [9,10]. Mutations such as L1213V, V1238I,

**Abbreviations:** 3-D, 3-dimensional; APG, Apigenin; GAPDH, Glyceraldehyde-3-phosphate dehydrogenase; HGF, hepatocyte growth factor; HRP, horseradish peroxidase; hrs, hours; IC<sub>50</sub>, half maximal inhibitory concentration; IL3, interleukin 3; mTOR, mechanistic target of rapamycin pathways; PAINS, pan-assay interference compounds; RCC, renal cell carcinoma; RTK, receptor tyrosine kinase; TPR, translocated promoter region; VHL, Von Hippel-Lindau disease tumor suppressor; WT, wild-type.

\* Corresponding author.

E-mail address: [xukp395@csu.edu.cn](mailto:xukp395@csu.edu.cn) (K. Xu).

<sup>1</sup> Jing Li and Guishan Tan contributed equally to this work.

<https://doi.org/10.1016/j.bcp.2021.114620>

Received 23 February 2021; Received in revised form 20 May 2021; Accepted 20 May 2021

Available online 24 May 2021

0006-2952/© 2021 Elsevier Inc. All rights reserved.

D1246N, Y1248H, or M1268T, were found in hereditary and sporadic papillary RCC [9,10]. These mutant MET display constitutive tyrosine phosphorylation [11], and are resistant to approved MET kinase inhibitor Cabozantinib, Capmatinib or Crizotinib [12–15]. In fact, mutant MET was more easily activated by HGF and stay activated for longer time than wild-type (WT) MET [16]. These mutations, coupled with the high expression of HGF in the kidney might explain why patients with germline MET mutation more likely have kidney cancer [5]. *In vitro* and *in vivo* studies demonstrated that the inactivation of VHL might increase MET expression in clear cell RCC [17–19]. Furthermore, phosphorylated MET was higher in RCC tumors [20,21], and indeed MET phosphorylation was correlated with greater proliferation index, greater tumor diameter, and worse cause-specific survival [21].

APG is a natural flavone, and is abundant in vegetables, fruits and herbs. In addition to anti-inflammation and anti-oxidation, the most widely studied function of APG is its anti-cancer activity against a variety of tumors including skin, breast, prostate, digestive tract, and certain hematological malignancies [22]. At the molecular level, APG was indicated to target a variety of proteins and signaling pathways directly or indirectly. A number of studies have illustrated that APG can inhibit the signaling pathways such as PI3K-Akt, JAK-Stat, WNT- $\beta$ -catenin and NF- $\kappa$ B [22], which are all involved in carcinogenesis and metastasis. APG can also directly bind to hnRNP2 and inhibit its dimerization and function [23]. PDGFR and Src kinase were also thought to be targets of APG [24–26]. However, the further development of APG for cancer therapy has been challenging since it has sub-optimal efficacy and bioavailability [22]. Nevertheless, efforts and progress have been made recently [27,28].

Whether APG has direct inhibitory activity against MET has not been conclusive. One study reported that high concentrations of APG inhibited MET phosphorylation [29]. In addition, other compounds with structural similarities to APG, such as Rutin, Isoquercitrin and Nobiletin, were reported to inhibit MET phosphorylation [30–32]. Yet another study indicated that APG had no effect on phosphorylated MET in MDA-MB-231 cells stimulated by HGF [33]. These inconclusive results could be due to the lack of potency of APG.

Anti-tumor effects of APG on RCC has not been widely studied. APG was found to have anti-RCC activity *in vitro* and *in vivo* through inducing cell cycle arrest and apoptosis [34]. Other APG-like compounds such as Vitexin and Scutellarin were shown to suppress RCC through inhibition of P13K-AKT-mTOR pathway [35,36]. To improve the activity of APG and to further study its anti-RCC activity, we modified the peripheral substituents of APG while keeping its core ring structure unchanged. Hence, a series of APG derivatives were synthesized and screened for their activity on a RCC cell line Caki-1 which carries a Cabozantinib-resistant V1238I mutation in MET [15]. We discovered that compound **15e** is most potent in inhibiting Caki-1 cell proliferation among APG and its derivatives and is superior to Crizotinib and Cabozantinib. Further mechanism studies indicated that **15e** directly targeted MET, and inhibited its kinase activity and downstream signaling. Importantly, **15e** inhibited mutant MET with V1238I and Y1248H mutations that are

resistant to current drugs. In addition, in an *in vivo* mice tumor model, **15e** repressed RCC growth through inhibition of MET activation. In summary, we identified an APG derivative, **15e**, which has the potential to be developed against RCC via a mechanism of directly targeting MET.

## 2. Materials and methods

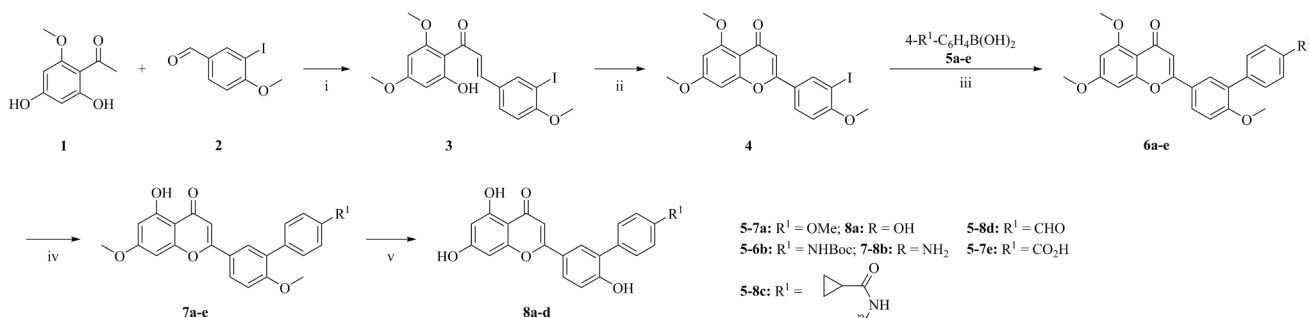
### 2.1. Materials in chemistry

Solvents and reagents were commercially available and used without further purification, unless otherwise stated. All reactions were monitored by thin layer chromatography (TLC) on silica gel GF254 (0.25 mm, Qingdao Ocean Chemical Ltd., China). Flash chromatography was performed using silica gel 60 (230–400 mesh, Qingdao Ocean Chemical Ltd., China). The purities of all target compounds were estimated by Waters 1525 Binary HPLC Pump.  $^1\text{H}$  NMR and  $^{13}\text{C}$  NMR spectra were recorded with an Agilent NMR Inova 400 or 600 spectrometer with TMS as the internal standard. All chemical shift  $\delta$  was given in parts per million (ppm). Mass spectra were recorded on an Agilent HPLC1260-MS6120 with ESI source as ionization, respectively. Chemical raw materials (**1**, **2** and **9**) were provided by Bidepharm, Shanghai, China. Apigenin and Crizotinib were purchased from MedChemExpress (HY-N1201, China) and Selleck (S1068, China).

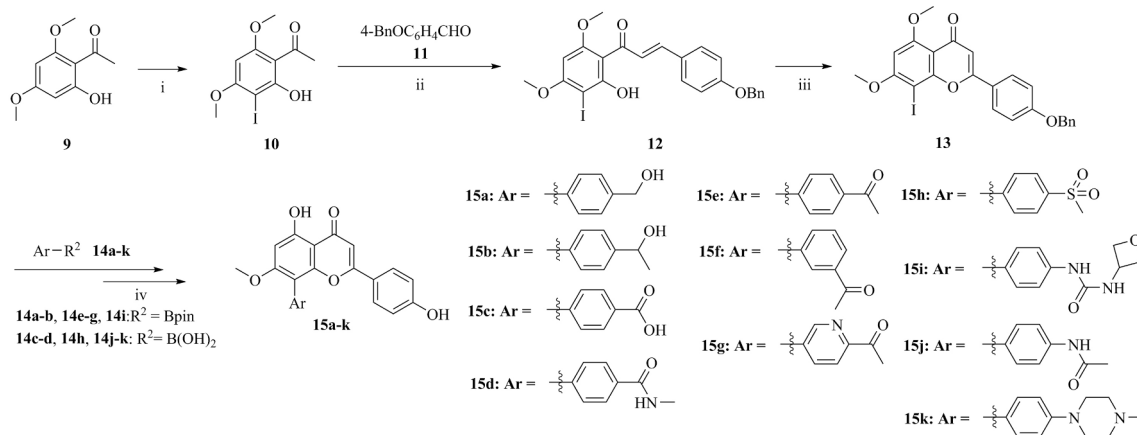
### 2.2. Synthetic route

The general synthetic routes of novel 5,7-dihydroxy-2-(6-hydroxy-[1,1'-biphenyl]-3-yl)-4H-chromen-4-one derivatives were illustrated in Scheme 1 [37,38]. The commercially material 1-(2,4-dihydroxy-6-methoxyphenyl) ethan-1-one (**1**) was treated with 3-iodo-4-methoxybenzaldehyde (**2**) in potassium hydroxide solution to give (E)-1-(2-hydroxy-4,6-dimethoxyphenyl)-3-(3-iodo-4-methoxyphenyl)prop-2-en-1-one (**3**), which was reacted with iodine to obtain compound **4**. Subsequently, compounds **6a-e** were prepared through Suzuki-Miyaura coupling reaction of compound **4** with boron reagents. Then, two-step demethylative reactions were performed to achieve the target products (**8**).

The general synthetic routes of novel 5-hydroxy-2-(4-hydroxyphenyl)-7-methoxy-8-phenyl-4H-chromen-4-one derivatives were illustrated in Scheme 2 [39,40]. The commercially material 1-(2-hydroxy-4,6-dimethoxyphenyl)ethan-1-one (**9**) was treated with iodine to obtain compound **10**, which was reacted with 4-(benzyloxy)benzaldehyde (**11**) in potassium hydroxide solution to give (E)-3-(4-(benzyloxy)phenyl)-1-(2-hydroxy-3-iodo-4,6-dimethoxyphenyl)prop-2-en-1-one (**12**). Next, a cyclization reaction was proceeded to achieve 2-(4-(benzyloxy)phenyl)-8-iodo-5,7-dimethoxy-4H-chromen-4-one (**13**). Subsequently, compounds **15a-k** were prepared through Suzuki-Miyaura coupling and deprotection reactions.



**Scheme 1.** Reagents and conditions: i) KOH (30 wt%), EtOH; ii)  $\text{I}_2$ , DMSO, 110 °C; iii)  $\text{Pd}(\text{PPh}_3)_4$ ,  $\text{Cs}_2\text{CO}_3$ , DMF/ $\text{H}_2\text{O}$ , 110 °C, iv)  $\text{AlCl}_3$ , 85 °C; v)  $\text{BBr}_3$ , rt.



**Scheme 2.** Reagents and conditions: i) I<sub>2</sub>, HNO<sub>3</sub>, EtOH; ii) KOH (30 wt%), EtOH; iii) I<sub>2</sub>, DMSO, 110 °C; iv) Pd(PPh<sub>3</sub>)<sub>4</sub>, Cs<sub>2</sub>CO<sub>3</sub>, DMF/H<sub>2</sub>O, 110 °C; AlCl<sub>3</sub>, 85 °C; BBr<sub>3</sub>, rt.

### 2.3. Cell culture

Cell lines in this investigation include following: human RCC cell line Caki-1 (ATCC, HTB-46), Caki-2 (ATCC, HTB-47), and ACHN (ATCC, CRL-1611); human lung cancer cell line NCI-H441 (ATCC, HTB-174) and NCI-H446 (ATCC, HTB-171); human gastric carcinoma cell line SNU-5 (ATCC, CRL-5973); human breast cancer cell line MCF7 (ATCC, CRL-3435) and MDA-MB-231 (ATCC, HTB-26); human melanoma cell line SK-MEL-28 (ATCC, HTB-72); mouse pro-B cell line Ba/F3 (DMSZ, CM-1517); mouse embryonic fibroblast cell line NIH-3T3 (ATCC, CRL-1658); human embryonic kidney cell 293T (ATCC, CRL-3216). For cell culture, SK-MEL-28, MDA-MB-231, Ba/F3 and SNU-5 cells were incubated in RPMI 1640 (HyClone, SH30809.01B) and the other cell lines were cultured in DMEM (HyClone, SH30243.01B) at 37 °C with 5% CO<sub>2</sub>. RPMI 1640 and DMEM were supplemented with 10%(v/v) fetal bovine serum (Gibco, 10091148) and 1%(v/v) penicillin–streptomycin (HyClone, SV30010). All cell passages were kept under 20.

### 2.4. Cell viability assay

Cell viability assay kit was purchased from Dojindo Molecular Technologies (CK04). The assay was performed according to the technical manual. Briefly, 6 × 10<sup>3</sup> cells were plated into 96-well dishes and incubated with different concentrations of compounds for 72 h (hrs). 10% (v/v) final concentration of CCK-8 buffer was then added and the cell were further cultured for 1–2 h before measurement of absorbance at 450 nm using a microplate reader. This assay was repeated three times.

### 2.5. Colony formation assay

1 × 10<sup>3</sup> cells were plated into 12-well dishes and cultured at 37 °C with 5% CO<sub>2</sub> for 24 hrs before the indicated dose of chemical compound was added and the cells were incubated for about 7 days before the a colony was stained using 0.5% crystal violet solution (Beyotime, C0121). Colony formation assay was repeated three times.

### 2.6. Growth of Caki-1 cell 3-dimensional (3-D) microsphere

4 × 10<sup>3</sup> Caki-1 cells per well were seeded in U-bottom 96-well dishes (ThermoFisher Scientific, 168136) and cultured for 4 days to form 3-D microspheres. 15e or APG (MCE, HY-N1201) were then added and the microsphere were further incubated for another 8 days before being photographed under microscopy (Nikon, Ts2R-FL) at 100×. This experiment was repeated three times.

### 2.7. Phospho-RTK assays

Phosphorylated RTKs were measured with the Human Phospho-RTK Array Kit (ARY001B) from R&D Systems according to the manufacturer's instructions. Briefly, 80% confluence Caki-1 cells in 10-cm dishes were treated with the indicated concentration of compound for 24 hrs. Cells were lysed with lysis buffer and protein concentration of the lysate was measured by BCA kit (ThermoFisher Scientific, 23225). Aliquots of 300 μg lysate was added to each well and incubated at 4 °C overnight on a shaker. After washes, anti-phospho-tyrosine-HRP detection antibody within the kit was added to each well and incubated at room temperature for 2 hrs on a shaker. Then the arrays were incubated with Chemi Reagent Mix and photographed with chemiluminescence system (BioRad, ChemiDoc XRS+). Phospho-RTK assay was repeated two times.

### 2.8. Apoptosis assay

2 × 10<sup>5</sup> Caki-1 cells seeded into 6-well dishes were incubated for 24 hrs before indicated concentrations of compounds were added for another 24 hrs incubation. Then, the cells were digested and suspended, washed with PBS twice and stained with Annexin V-FITC and PI staining buffer (Dojindo Molecular Technologies, AD10) for 30 min at 37 °C. The resulting samples were analyzed by flow cytometry using Beckman Cytoflux. Apoptosis assay was repeated three times.

### 2.9. Cell cycle assay

2 × 10<sup>5</sup> Caki-1 cells were seeded into 6-well dishes and incubated for 24 hrs before culture medium was replaced with fresh medium containing compounds and incubated for another 24 hrs. The cells were then harvested, washed with ice-cold PBS and fixed with ice-cold 70% ethanol at 4 °C for 12 hrs before stained with PI staining buffer (Beyotime, C1052) for 30 min at 37 °C. The resulting samples were analyzed by flow cytometry using Beckman Cytoflux. Cell cycle assay was repeated three times.

### 2.10. Immunoblot

2 × 10<sup>5</sup> Cells were seeded in 6-well dishes overnight prior to treatment with the indicated concentrations of compound. Cells were quickly lysed by adding 200 μL 2 × SDS buffer, and then collected and incubated at 95 °C for 5 min. The proteins were separated on SDS-PAGE (sodium dodecyl sulfate–polyacrylamide gel electrophoresis) and transferred to polyvinylidene fluoride membranes (BioRad, 1620177). The membranes were blocked with 5% BSA/PBST buffer at room temperature for 1 h and then incubated at 4 °C overnight with primary antibodies in 5%

BSA/TBST buffer with gentle shaking. Primary antibodies in the research were purchased from Cell Signaling Technologies, including MET (#8198), p-MET-Y1234/Y1235 (#3077), Akt (#2920), p-Akt-S473 (#4060), p-Akt-T308 (#4056), Stat3 (#9139), p-Stat3-Y705 (#9145), Erk1/2 (#4696), p-Erk1/2-T202/Y204 (#4370), PRAS40 (#2691), p-PRAS40-T246 (#2997), mTOR (#2983), p-mTOR-S2448 (#5536), p70-S6K (#2708), and p-p70-S6K-T389 (#9234). All primary antibodies were 1:1000 diluted in PBST buffer (PBS + 0.5%(v/v) Tween-20) with 5% BSA. After the primary antibodies incubation, the membranes were washed with PBST three times and incubated with appropriate peroxidase-conjugated secondary antibodies (anti-IgG-HRP, 1:5000, CST, #7074, or #7076) for 1 h at room temperature and washed again. Protein bands were visualized using enhanced ECL western blotting detection reagents (ThermoFisher Scientific, SuperSignal West Dura, 34076) followed by capturing photos with chemiluminescence system (BioRad, ChemiDoc XRS+). Bands in these photos were quantified through measuring gray value with Image J (NIH). Each immunoblot was repeated at least three times.

### 2.11. Plasmids, siRNA and transfection

Service of gene synthesis, gene clone and mutation, and siRNA was all purchased from Synbio Technologies (Suzhou, China). cDNA of TPR-MET, and WT or mutant MET (isoform 2) were inserted into vector pLVX-IRES-Puro (Takara, 631253) and pCDNA3.1 (ThermoFisher Scientific, V790-20) respectively. The sequences of si-MET were 5'-CAUCCAGAAUGUCAUUCUAdTdT-3' and 5'-UAGAAUGACAUCUGGAUGdTdT-3'; The sequences of si-NC (siRNA negative control) were 5'-UUCUCCGAACGUGUCACGUDtT-3', and 5'-ACGUGACACGUUCGGAGAAdTdT-3'. 80% confluence NIH-3T3 cells or Caki-1 cells in 6-well dishes were transfected with 1 µg MET plasmid or 60 pmol siRNA respectively by using lipofectamine 3000 (ThermoFisher Scientific, L3000008). 24 hrs later, cells were digested and suspended, and  $1 \times 10^5$  NIH-3T3 cells per well were seeded into 24-well dishes and treated with **15e** for 24 hrs before cells were lysed with 100 µL  $2 \times$  SDS for immunoblot analysis. si-RNA transfected Caki-1 cells were seeded into 96-well dishes and treated with the indicated concentrations of **15e** for 72 hrs before the cell viability was assessed by using CCK-8 assay kit.

### 2.12. Lentivirus preparation and Ba/F3-TPR-MET stable cell-line establishment

90% confluence 293 T cells in 6-well dishes were transfected with 2 µg lentivirus vector, 2 µg psPAX2 (Addgene, 12260) and 0.5 µg pMD2.G (Addgene, 12259) through lipofectamine 3000 (ThermoFisher Scientific, L3000008). 24 hrs later, culture medium was replaced with 2 mL 20%-FBS-containing DMEM, and the transfected cells continued to being cultured for another 48 hrs until the culture medium was collected and filtered with 0.22 µm filter (Millipore, SLGP033RB). Filtered medium with lentivirus then was used to incubate Ba/F3 cells for 24hrs. Finally, infected Ba/F3 cells were cultured in medium without interleukin 3 (IL3) for 9 days and then in medium with 0.5 µg/mL puromycin (Gibco, A1113803) for 4 days.

### 2.13. Wound healing assay

$2 \times 10^5$  Caki-1 cells were seeded per well in 6-well dishes and incubated for 48 hrs until they reached 80%–90% confluence. A confluent monolayer of Caki-1 cells was artificially wounded with a micropipette tip, and the detached cells were washed with PBS and treated with vehicle or indicated compounds in growing medium for 24 hrs. Images of the wounds were photographed at 0 and 24 hrs under microscope (Nikon, Ts2R-FL) at 100 $\times$ . This experiment was repeated three times.

### 2.14. Trans-well migration assay

$7 \times 10^4$  cells in FBS-free DMEM with different concentrations of compounds were seeded into the upper apartment of 8 µm pores trans-well device (Corning, 3422) containing 500 µL 10%-FBS-containing DMEM with or without 15 ng/mL HGF (R&D Systems, 294-HG) in the lower apartment. After the device was incubated at 37 °C with 5% CO<sub>2</sub> for 16 hrs, cells in upper wells were completely removed with cotton swabs. Cells that had migrated to the lower surface of the filters were fixed with methanol and stained with crystal violet (Beyotime, C0121). Finally cells migrated to the lower surface of the filters were photographed under microscopy at 100 $\times$ . This experiment was repeated three times.

### 2.15. Molecular docking

The crystallography structure of MET was downloaded from the Protein Data Bank (<http://www.rcsb.org>, PDB code 3F66). All water molecules were deleted. The protein structure was prepared using the Schrödinger's Protein Preparation Wizard (Schrödinger Release 2018-1: Schrödinger Suite 2018-1 Protein Preparation Wizard; Epik, Schrödinger, LLC, New York, NY, 2016; Impact, Schrödinger, LLC, New York, NY, 2016; Prime, Schrödinger, LLC, New York, NY, 2018.) in Maestro version 11.5. The molecular structure of **15e** was generated using Schrödinger's 3D Builder tool and the ligand was prepared using the Schrödinger's LigPrep tool (Schrödinger Release 2018-1: LigPrep, Schrödinger, LLC, New York, NY, 2018.). The receptor grids for the docking procedure were generated using the native ligand of the crystal structure as the centroid of the grid box. **15e** was docked into the prepared protein using Glide (Schrödinger Release 2018-1: Glide, Schrödinger, LLC, New York, NY, 2018.) in the extra precision (XP) mode. The number of poses per ligand to include in the postdocking minimization step was set to 100, and the maximal number of docking poses output for the ligand was set to 20.

### 2.16. In vivo xenograft tumor experiment

Four-week-old female athymic nude mice (BALB/c-nu) were purchased from Hunan SJA Laboratory Animal Co., LTD. Mice were housed under standard conditions with freedom to water and food, and were subjected to a 12-hour light/dark cycle. All mice protocols were approved by the Animal Ethics Committee at the Sunshine Lake Pharma Co., LTD (Dongguan, China) and were in compliance with Chinese Association for Laboratory Animal Sciences guidelines. Caki-1 cell suspension ( $1 \times 10^7$  cells in 200 µL of medium) was injected subcutaneously into the right flank of each mouse on day 0. When the tumor volume reached 200 mm<sup>3</sup> the mice were randomized into vehicle control and treatment groups (6 animals per group). 20 mg/kg **15e** or APG (in 200 µL of vehicle solution (5% DMSO and 15% PEG400 in saline, pH 9) was administered daily by intraperitoneal injection for 16 days while the control group was treated with an equal volume of vehicle solution. The tumor weight was measured at the termination of the experiment and the body weight mouse was monitored throughout the experiment for toxicity.

### 2.17. Immunohistologic chemistry

Tumor tissues were sectioned and immunohistochemically analyzed for MET and p-MET-Y1234/Y1235 expression. Sections of the tumor tissues were incubated at 4 °C overnight with the antibodies for MET and p-MET-Y1234/Y1235, and detected using TMB Chromogen Solution (Beyotime, P0211). The stained section was observed under an inverted phase-contrast microscope and photographed.

## 2.18. Data statistics

Except phospho-RTK array, all experiments were performed at least three times, and representative data are shown. Statistical significance ( $p < 0.05$ ) was assessed using Student's *t* test or oneway ANOVA coupled with Dunnett's *t* test. Not significant (n.s.) indicated  $p > 0.05$ . All data were represented as means  $\pm$  SD.

## 3. Results

### 3.1. 1. Activity of APG derivatives against Caki-1 cell

The synthesized compounds (Fig. 1) were evaluated by CCK-8 assay, and were compared with Crizotinib as positive control. In CCK-8 assay, Caki-1 cells were treated with APG or its derivatives for 72 hrs before cell viability was measured. Then half maximal inhibitory concentration ( $IC_{50}$ ) on cell viability was calculated and shown in Table 1, where the synthesized compounds displayed moderate to high potency against Caki-1 cell viability. Compound 15e with a para-acetylphenyl nonpolar group was the most potent compound to affect Caki-1 cell viability. Interestingly, the  $IC_{50}$  of 15e is 10 times better than Crizotinib (Table 1), and is also better than the reported  $IC_{50}$  (14.5  $\mu$ M in Caki-1 cell) for the approved RCC drug Cabozantinib [15].

### 3.2. In vitro activity of the APG derivative 15e against RCC cell growth

To further study and compare 15e and APG with Crizotinib for their inhibition activity on RCC and to ascertain the observed effect with Caki-1 can be extended to two other RCC cell lines, Caki-2 and ACHN, were further selected and investigated for their susceptibility to the compounds. As shown in Fig. 2A, all three cell lines showed similar cell viability profiles demonstrating that the inhibition is not limited to Caki-

**Table 1**

$IC_{50}$  of Caki-1 cells treated with APG and its derivatives.

Compounds	$IC_{50} \pm SD$ ( $\mu$ M) <sup>a</sup>
APG	44.27 $\pm$ 2.02
Crizotinib	4.43 $\pm$ 0.22
8a	>50
8b	>50
8c	28.57 $\pm$ 1.79
8d	>50
7d	>50
7e	>50
15a	26.78 $\pm$ 1.49
15b	5.66 $\pm$ 0.17
15c	>50
15d	>50
15e	0.49 $\pm$ 0.02
15f	>50
15g	>50
15h	7.84 $\pm$ 0.99
15i	11.02 $\pm$ 1.26
15j	4.51 $\pm$ 0.08
15k	24.64 $\pm$ 1.71

<sup>a</sup>. The average value of the three independent experiments was expressed by mean  $\pm$  SDs.

1. In addition, 15e showed a remarkable improvement of anti-proliferative activity over APG and Crizotinib in all three cell lines. For later studies, Caki-1 cells were mainly used.

To re-confirm the ability of 15e in inhibiting Caki-1 cell growth, we performed colony-formation and 3-D cell microsphere growth assays. 0.625  $\mu$ M 15e clearly inhibited the formation of colonies and 5  $\mu$ M 15e or Crizotinib completely blocked the formation of colonies from Caki-1 cells, while 5  $\mu$ M APG had no effect on the colony-forming ability (Fig. 2B). Caki-1 cells formed 3-D microspheres after being cultured for

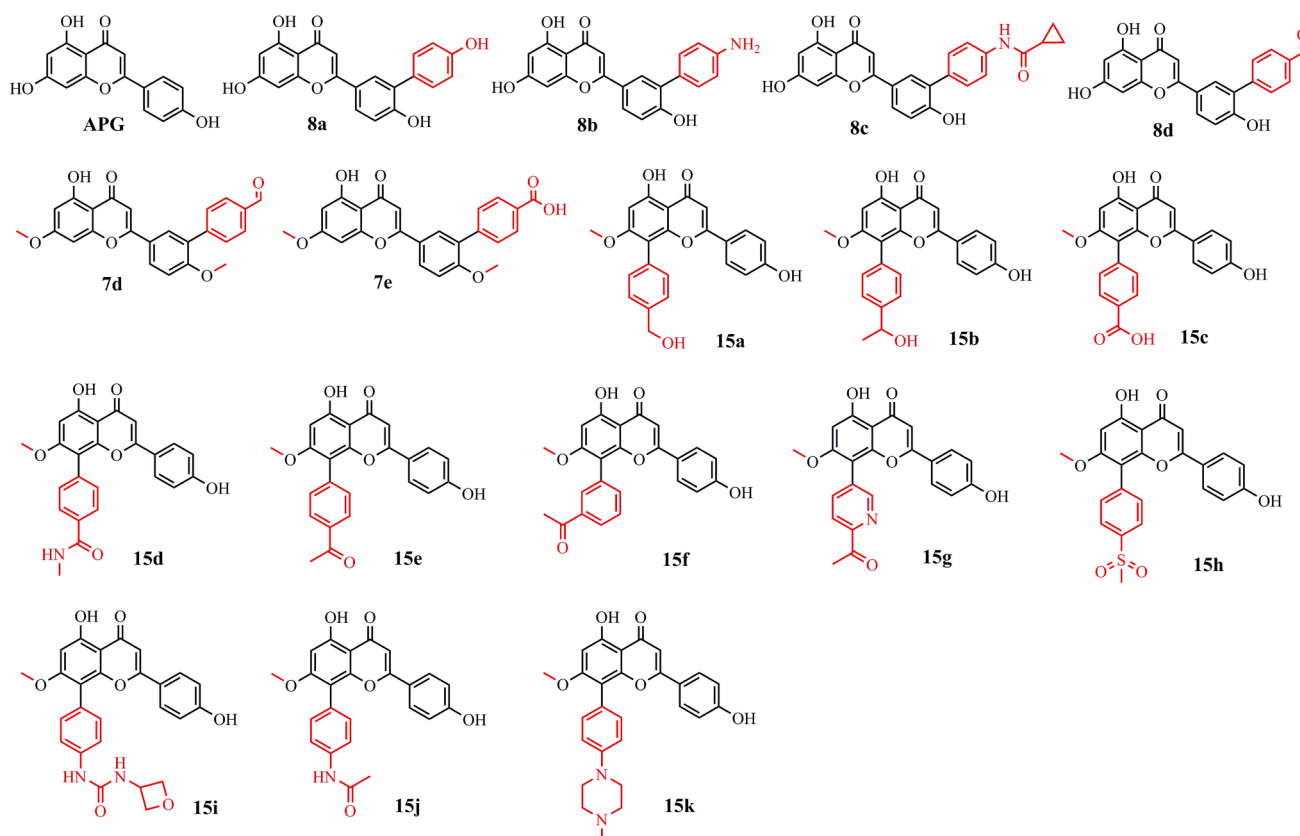


**Fig. 1.** The structures of APG and its novel synthesized derivatives. Structural changes are highlighted in red. (For interpretation of the references to color in this figure legend, the reader is referred to the web version of this article.)

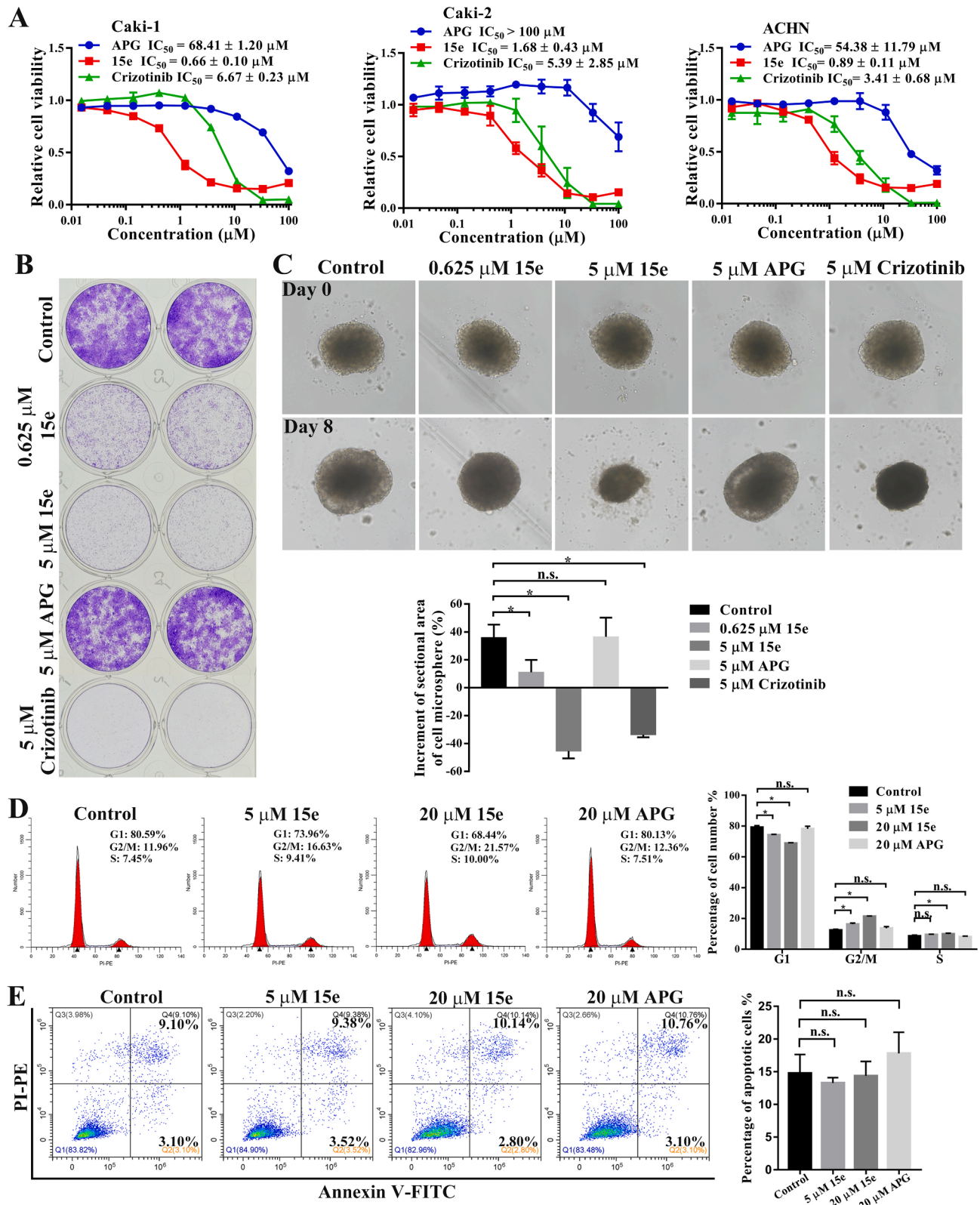


**Fig. 2.** *In vitro* anti-tumor effects of APG derivative 15e. (A) Relative cell viability of Caki-1, Caki-2 and AHCN cells treated with 0.01–100 μM 15e, APG or Crizotinib for 72 hrs. (B) Colony-forming ability of Caki-1 cells or (C) Growth of Caki-1 cell 3-D microsphere treated with vehicle, 0.625 μM 15e, 5 μM 15e, 5 μM APG or 5 μM Crizotinib for 8 days respectively. The growth of Caki-1 cell 3-D microsphere was quantified by calculating the increment of sectional area of cell microspheres. (D) Cell cycle analysis and (E) apoptosis assays of Caki-1 cells treated with indicated concentration of 15e or APG for 24 hrs. Data are expressed as the mean ± SD, n = 3, \*P < 0.05 versus Control. Not significant (n.s.) indicated P > 0.05.

4 days in a 96-well U-bottom dish (Fig. 2C, Day 0) and they can grow bigger after another 8-day incubation (Fig. 2C, Day 8). When 15e or APG was added during the 8-day incubation period, the growth of cell microspheres was significantly repressed by 5  $\mu$ M 15e and Crizotinib but not by APG (Fig. 2C).

Loss of cell viability measured by CCK8 can be due to cell death or lack of cell proliferation. Hence, assays for apoptosis or cell cycle were employed to check whether 15e could function with either of these two aspects. When exponentially growing Caki-1 cells were incubated with 5  $\mu$ M or 20  $\mu$ M 15e, cells at G2/M increased indicating that the cell cycle was blocked at this phase (Fig. 2D). Even at 20  $\mu$ M, APG did not affect the cell cycle, demonstrating the improvement in 15e activity. To assess whether 15e is simply cytotoxic and causing cell death, apoptosis of Caki-1 cells in the presence or absence of compounds was investigated by flow cytometry. Neither 15e nor APG caused significant apoptosis (Fig. 2E).

### 3.3. 15e inhibits Caki-1 cell migration and invasion *in vitro*

Given the above results, we further tested whether 15e can affect Caki-1 cell migration and invasion in a wound healing assay and a trans-well chamber assay, respectively. 15e at 0.625 and 5  $\mu$ M effectively blocked wound closure of Caki-1 cells (Fig. 3A). Similarly, in trans-well chamber assay, treatment with 15e significantly decreased the number of Caki-1 cells invading to the *trans* surface of trans-well chambers (Fig. 3B). In both assays, however, APG had minimum effect, again demonstrating the improvement of 15e.

### 3.4. Anti-proliferation activity of 15e correlates to phosphorylated MET

Previously, APG was thought to have inhibitory activity against

cellular kinases [24,26,29,41]. Therefore, to explore the molecular targets and mechanism of action of the anti-tumor activity of 15e against Caki-1 renal cancer cell, we screened a panel of 49 different RTKs by using a phospho-RTK array to detect which kinase is the target of 15e. Specific RTK capture antibodies were spotted in duplicate on the array, so when a cell lysate is applied to the array, RTKs, both phosphorylated and un-phosphorylated, will be captured. A second anti-phosphotyrosine antibody conjugated to horseradish peroxidase (HRP) is then applied to detect the presence and the abundance of that specific phosphorylated kinase. As shown in Fig. 4A, lysates from Caki-1 cells contained a variety of detectable phosphorylated RTK and can be detected using this array, for example MET, EGFR, PDGFR $\beta$  and Ryk, at the experimental conditions. Treatment of Caki-1 cells with 5  $\mu$ M 15e for 24 hrs, however, affected the amount of several phospho-RTKs with phospho-MET the most significantly decreased (Fig. 4A). Quantification of the phospho-RTK array showed that 15e decreased phospho-MET to 1/6 of that in the control group (Fig. 4B).

The above data suggest that tyrosine kinase MET could be the direct target for 15e, since MET is auto-phosphorylated [8]. If this hypothesis is true, cells with high MET expression should be more affected by 15e. To test this idea, seven different cancer cell lines with different levels of MET and phosphorylated MET (Y1234/Y1235) were selected and tested for their sensitivity to 15e. Caki-1, lung cancer cell NCI-H441 and gastric carcinoma cell SNU-5 expressed high levels of total MET and phosphorylated MET (Y1234/Y1235), while breast cancer cell MCF7 and MDA-MB-231, small cell lung cancer cell NCI-H446 and melanoma cell SK-MEL-28 had low MET and phosphorylated MET expression (Fig. 4C and D). Indeed, though there is considerable variation, Caki-1, NCI-H441 and SNU-5 cells are very sensitive to 15e with IC<sub>50</sub> 0.60, 0.45 and 3.92  $\mu$ M, respectively. In stark contrast, the other cells were all less responsive to 15e treatment with IC<sub>50</sub> exceeding 10  $\mu$ M (Fig. 4E and F).

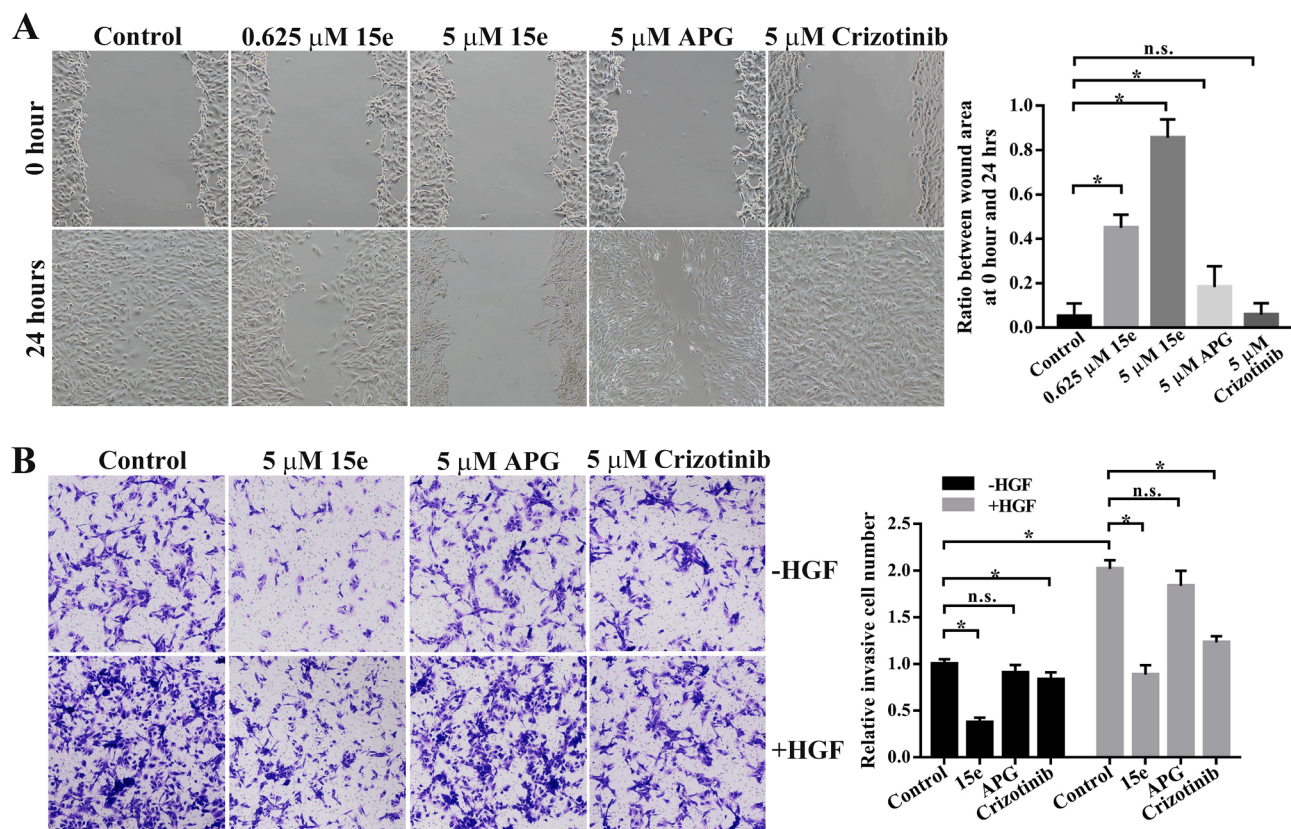
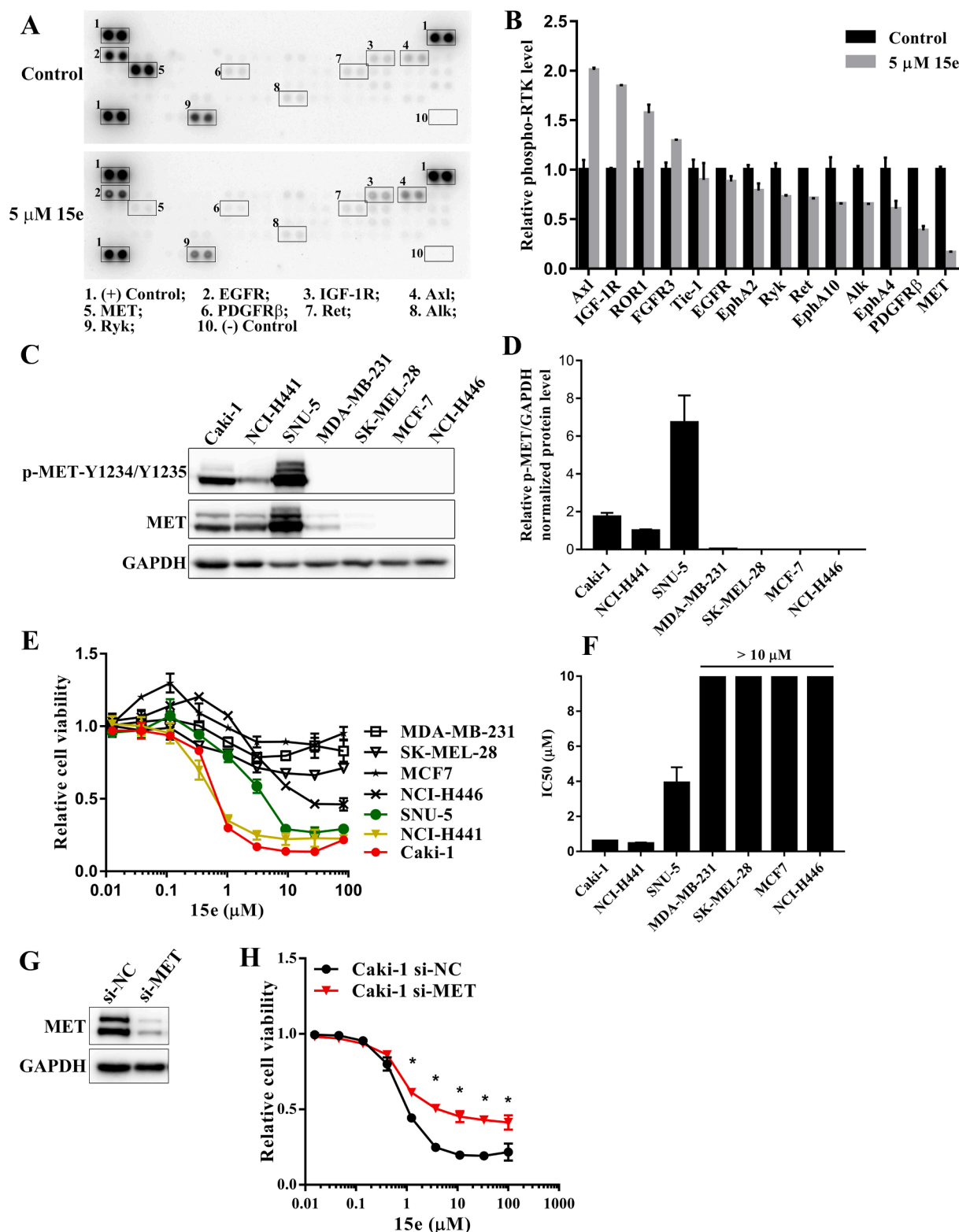


Fig. 3. 15e inhibits Caki-1 cell migration and invasion *in vitro*. (A) Wound healing assays of Caki-1 cells treated with vehicle, 0.625  $\mu$ M 15e, 5  $\mu$ M 15e, 5  $\mu$ M APG or 5  $\mu$ M Crizotinib. (B) Trans-well chamber assays of Caki-1 cells treated by vehicle, 5  $\mu$ M 15e, 5  $\mu$ M APG or 5  $\mu$ M Crizotinib along with or without 15 ng/mL HGF. Data are expressed as the mean  $\pm$  SD, n = 3, \*P < 0.05 versus Control. Not significant (n.s.) indicated P > 0.05.



**Fig. 4.** 15e induced anti-proliferation correlates to phosphorylated MET. (A) Phospho-RTK arrays of Caki-1 cells treated with vehicle or 5  $\mu$ M 15e for 24 hrs. Several phosphorylated RTKs were marked with black framework and number as indicated. (B) Quantification of 14 detectable Phospho-RTK expression in the assay of phospho-RTK arrays. (C) Protein level of total MET and phosphorylated MET, and (D) quantification of relative p-MET/GAPDH protein level in seven cancer cell lines. (E) Relative cell viability of seven cancer cell lines treated with 0.01–90  $\mu$ M 15e for 72 hrs and (F) their IC<sub>50</sub> statistics (n = 3). (G) MET expression in si-MET or si-NC transfected Caki-1 cells. (H) Relative viability of si-MET or si-NC transfected Caki-1 cells treated with 15e. Data are expressed as the mean  $\pm$  SD, n = 3, \*P < 0.05 versus si-NC.

The variation of IC<sub>50</sub> in Caki-1, NCI-H441 and SNU-5 cells could be contributed by the growth conditions of the different cancer cells.

To further confirm that it is the MET dependent cell growth of Caki-1 that was inhibited by **15e**, we thought that knock down MET in Caki-1 cells with siRNA will decrease the inhibition by **15e**. To that end, we knocked down MET (Fig. 4G) and examined the anti-proliferation activity of **15e**. The results in Fig. 4H showed that this is the case, as si-MET treated cells were less susceptible to **15e** than control si-NC treated Caki-1 cells. The data demonstrated that **15e** was targeting MET and inhibiting MET for inhibition of Caki-1 cell proliferation.

### 3.5. **15e** targets MET and inhibits its kinase activity

The decrease in phospho-MET seen in **15e** treated Caki-1 cells (Fig. 4A) could be due to decrease in MET protein or MET phosphorylation. To clarify this point, we conducted immunoblot to examine MET and Phospho-MET in **15e** treated Caki-1 and NCI-H441 cells directly. Phosphorylated MET (Y1234/Y1235), but not total MET, decreased with increasing concentrations of **15e** indicating that **15e** inhibited MET phosphorylation. As expected, the less active compound APG did not affect MET phosphorylation at the same concentration (Fig. 5A and B).

Since Y1234/Y1235 are auto-phosphorylated [7], **15e** was assumed to inhibit the MET auto-phosphorylation kinase activity. To further confirm this notion, we developed a Ba/F3 cell line, a mouse pro-B cell, whose growth is dependent on the presence of IL-3 [42], by introducing a *translocated promoter region (TPR)-Met* fusion gene to make the growth of the cell dependent on MET in the absence of IL-3 [43]. The TPR-MET contains a dimerization domain from TPR and a kinase domain from MET, so that TPR-MET is constitutively active because of the auto-dimerization [44]. In the Ba/F3 cells, inhibiting TPR-MET kinase activity will lead to the suppression of cell viability. As expected, **15e** was found to only potently inhibit Ba/F3-TPR-MET cells with an IC<sub>50</sub> 0.44 μM (Fig. 5C). The activity of **15e** was four times less in Ba/F3 cells in the presence of IL-3 (IC<sub>50</sub> = 1.69 μM). The original APG has much less activity in either cells (7.93 μM and 15.38 μM, respectively) (Fig. 5C). As expected, the MET phosphorylation in Ba/F3-TPR-MET cells were significantly inhibited by **15e** but not APG in a dose-dependent manner with western blot analysis (Fig. 5D, with quantitation in Fig. 5E). The results in this system further demonstrated that the target of **15e** is indeed MET.

Molecular docking of **15e** to the available crystal structure of MET kinase domain (PDB code 3F66) [45] further supported the above conclusion. Docking of **15e** (Fig. 5F) showed that **15e** can fit into the MET kinase pocket with the 5-hydroxyl-chromone group formed two hydrogen bonds with the kinase hinge region residue M1160. Moreover, the 5-hydroxyl-chromone group might also have hydrophobic interactions with side chains of residues I1084, Y1159 and M1211. The 4-hydroxy phenyl group could bind in the hydrophobic pocket surrounded by side chains of residues V1092, L1140, L1157 and Y1230 and has hydrogen bond with the hydroxy group of residue Y1230. The 4-acetyl phenyl group fits in the lipophilic pocket surrounded by residues M1211, Y1230 and D1231 (Fig. 5F).

### 3.6. **15e** downregulates MET downstream Akt and Stat3 signaling

As a receptor tyrosine kinase, MET was the upstream regulator of several classical downstream pathways including PI3K-Akt, Ras-Raf-MEK-Erk and Stat3 [8]. The effect of **15e** on the downstream three pathways were investigated in Caki-1 cells. Indeed, phosphorylated Akt (S473 or T308) and phosphorylated Stat3 (Y705), but not phosphorylated Erk1/2 (T202/Y204) were downregulated by **15e** in a dose-dependent manner (Fig. 6A and B). As expected when HGF was added to activate MET, Akt and Stat3 phosphorylation were increased and **15e** can still inhibit this HGF-induced enhancement of Akt and Stat3 phosphorylation (Fig. 6C and D). It indicated that **15e** can block the signaling from MET to Akt and Stat3.

We further investigated how **15e** affect the Akt kinase substrates PRAS40 [46] and downstream pathway mTOR-p70-S6K [46]. In Fig. 6E and F, phosphorylation of PRAS40, mTOR and p70-S6K were decreased in Caki-1 cells treated with **15e** in a dose-dependent manner.

### 3.7. Effects of **15e** on mutant MET

Mutations in MET that activate its activity are found in hereditary and sporadic papillary RCC. These include L1213V, V1238I, D1246N, Y1248H, or M1268T [9,10]. Among these, MET<sup>L1213V/D1246N/Y1248H</sup> are resistant to Crizotinib [14] and Capmatinib [13,14], and MET<sup>V1238I</sup> is resistant to Cabozantinib [15]. To investigate whether these mutant MET were also resistant to **15e**, we transfected mouse embryonic fibroblast NIH-3T3 cells with WT or mutant MET expressing plasmids and incubated with **15e** before detecting phosphorylation of MET. First, WT and mutant MET were expressed at similar levels. As expected, the mutant Met has higher kinase activity as shown by the higher levels of phosphorylated MET at Y1234/Y1235 (Fig. 7A). As shown by the immunoblot and quantification (Fig. 7B and C), **15e** was able to inhibit the kinase activity of MET<sup>V1238I</sup>, MET<sup>Y1248H</sup> and MET<sup>M1268T</sup> as well as MET<sup>WT</sup>, MET<sup>D1246N</sup>, and MET<sup>L1213V</sup> were also partially inhibited by **15e**. These data are significant as **15e** could potentially be further developed to treat Crizotinib, Capmatinib or Cabozantinib resistant patients who carry MET<sup>Y1248H</sup> or MET<sup>V1238I</sup> mutations. MET<sup>H112L</sup>, however, was resistant to **15e**.

### 3.8. **15e** inhibits tumor growth and MET phosphorylation *in vivo*

To examine the antitumor activity of **15e**, we conducted a xenograft tumor model in mice. Nude mice subcutaneously engrafted with Caki-1 cells were randomized and received intraperitoneal administration of vehicle, **15e** (20 mg/kg) or APG (20 mg/kg) for 16 days. At the termination of the experiment, tumor weight and body weight of the mice were measured, and tumors were photographed (Fig. 8A). The mean tumor weight of the vehicle control, **15e** and APG groups were 1.35 g, 0.52 g and 1.40 g, respectively, and the difference between the **15e** and control group was statistically significant ( $p < 0.05$ ) (Fig. 8B). There was no difference in body weight among the groups (Fig. 8C). These data demonstrate that **15e** can effectively inhibit the tumor growth of renal cancer cells *in vivo*.

The level of MET and phosphorylated MET in these tumor tissues were further assessed. Immunohistochemical staining of MET and p-MET-Y1234/Y1235 showed that while the total MET protein was not significantly decreased in the **15e** and APG treated mice, the phosphorylated MET at Y1234/Y1235 was visibly decreased in **15e** treated tumor tissues (Fig. 8D) while the decrease by APG is not obvious. These data are consistent with the *in vitro* data in cell lines.

## 4. Discussion

Despite nephrectomy with curative intent, about one third of patients with clear cell RCC develop metastases which are associated with high mortality [1]. Targeted therapies for RCC against VEGF and mTOR have been developed, but treatment response is varied and most patients eventually experience disease progression [47]. Therefore, there is still a tremendous unmet medical need for RCC. Although many studies have verified the anti-tumor activity of APG in different cancer cell lines, the activity of APG is usually too low to be further developed [22]. However, some studies reported that structural modification of APG can elevate its anti-proliferation activity in multiple cancer cell lines [27,28], and especially a APG derivative exhibited strong activity against colorectal adenocarcinoma (HT-29) and leucocythemia (HL-60) cells with IC<sub>50</sub> value of 2.03 μM and 2.25 μM, respectively, which were better than 5-fluorouracil [28]. Here we synthesized a series of novel APG derivatives with difference at the Ar group (Scheme 2) and found that a derivative **15e**, with a para-acetylphenyl nonpolar group, had potent

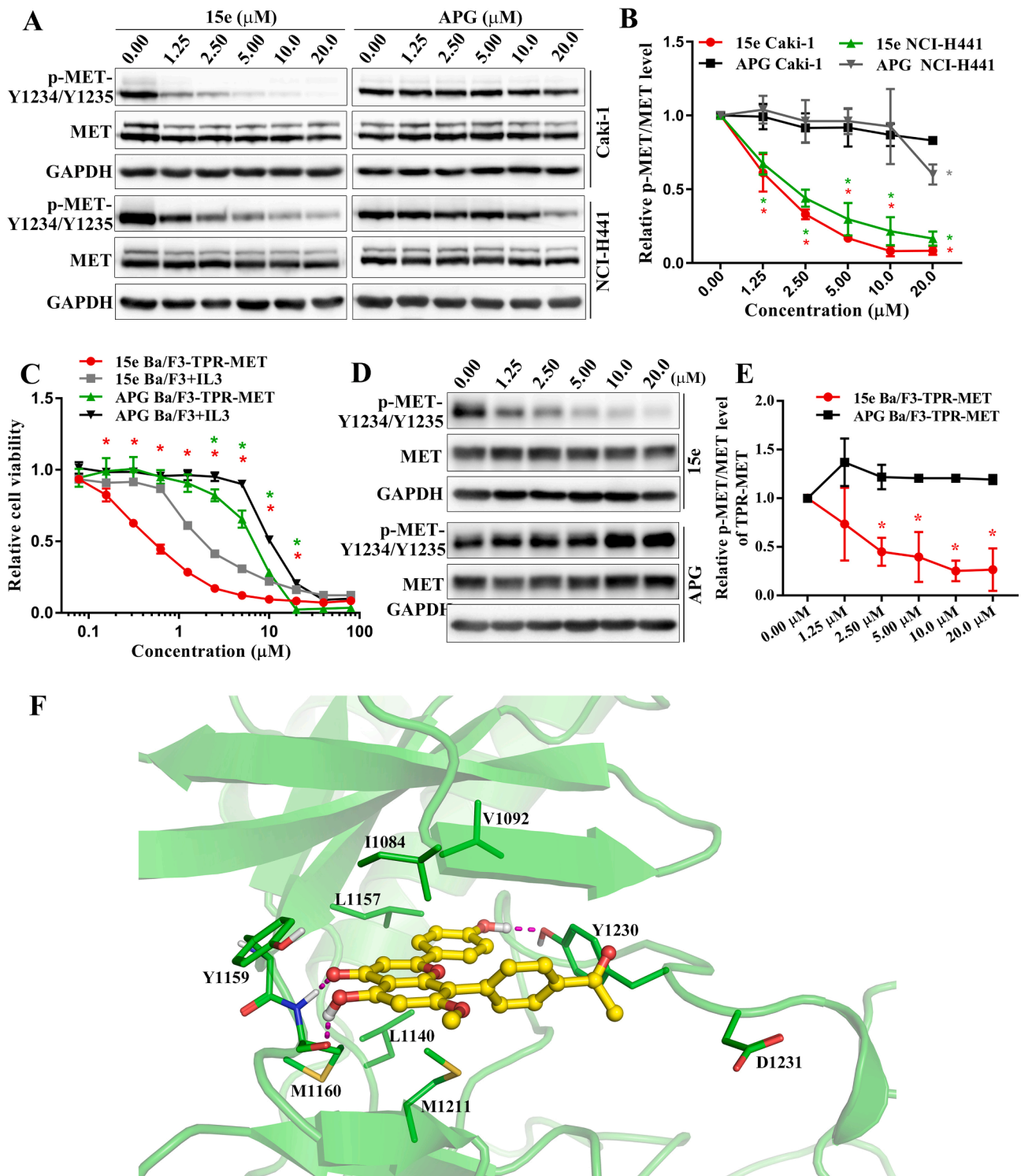


**Fig. 5.** 15e directly targets MET kinase domain and inhibits its kinase activity. (A) Immunoblot of MET and p-MET-Y1234/Y1235 in Caki-1 and NCI-H441 cells treated with 0 and 1.25–20  $\mu\text{M}$  15e or APG for 16 hrs. (B) Quantification of relative p-MET/MET protein level in (A). (C) Relative viability of Ba/F3-WT and Ba/F3-TPR-MET cells treated with concentration gradients of 15e or APG for 72 hrs. (D) Immunoblot and (E) its analysis of TPR-MET phosphorylation in Ba/F3-TPR-MET cells treated with indicated concentrations of 15e or APG. (F) 15e docked into the ATP-binding cleft of MET. 15e is shown as yellow ball and stick. The key amino acid residues are shown as green stick. Hydrogen bonds are shown as magenta dashed lines. Data are expressed as the mean  $\pm$  SD,  $n = 3$ , \* $P < 0.05$  versus Control (0  $\mu\text{M}$ ) in (B) and (E), or \* $P < 0.05$  versus group of Ba/F3 + IL3 in (C). (For interpretation of the references to color in this figure legend, the reader is referred to the web version of this article.)

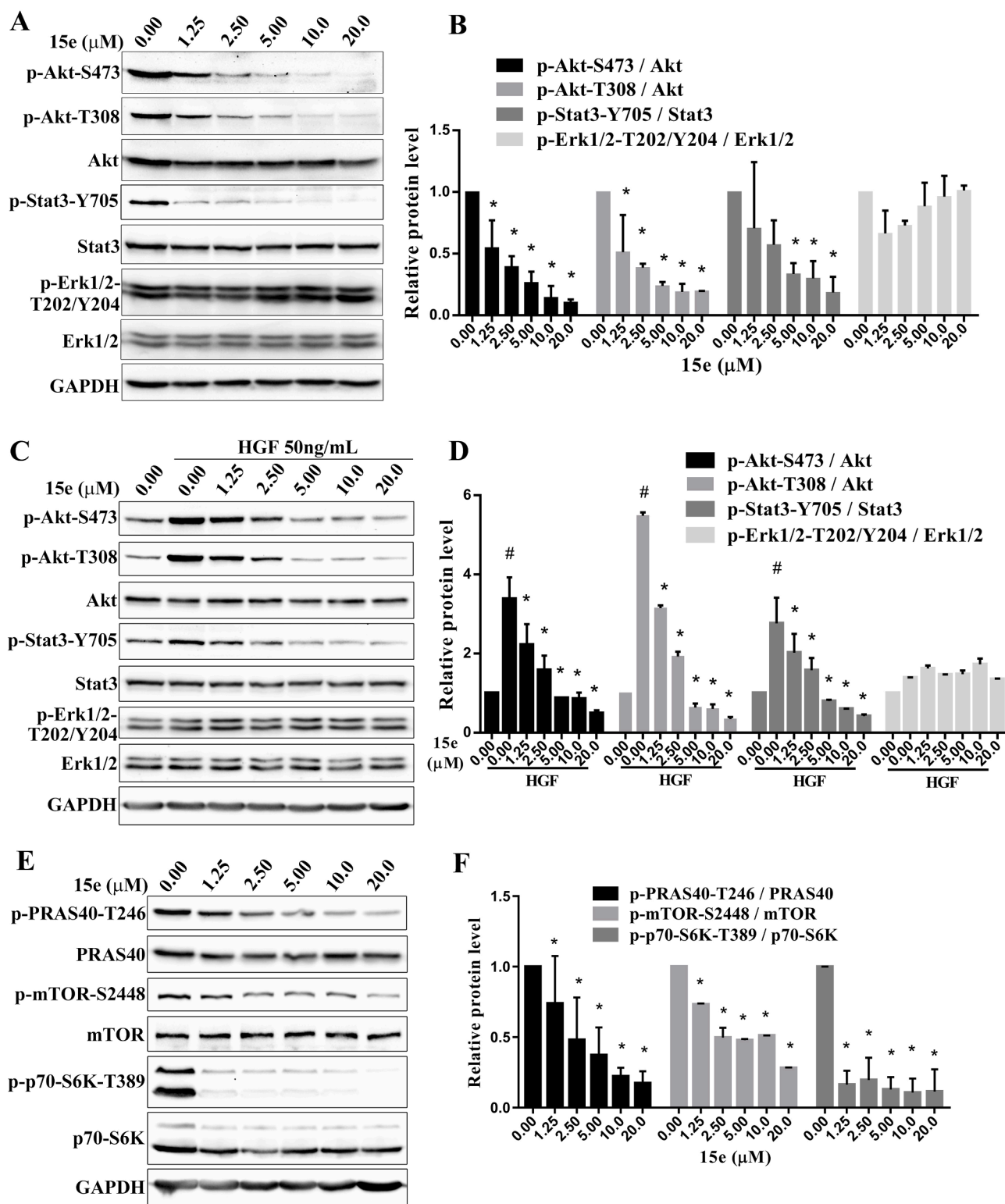


**Fig. 6.** 15e downregulates MET downstream Akt and Stat3 signaling. (A) Immunoblot analysis and (B) its quantification of MET downstream protein in Caki-1 cells treated with 0 and 1.25–20  $\mu\text{M}$  15e for 16 hrs. (C) Immunoblot analysis and (D) its quantification of MET downstream protein in HGF stimulated Caki-1 cells treated with 0 and 1.25–20  $\mu\text{M}$  15e. The cells were pre-incubated by 15e for 3 hrs before 50 ng/ml HGF stimulation for 15 min. (E) Immunoblot analysis and (F) its quantification of Akt downstream protein in Caki-1 cells treated with 0 and 1.25–20  $\mu\text{M}$  15e for 16 hrs. Data are expressed as the mean  $\pm$  SD,  $n = 3$ , \* $P < 0.05$  versus group of 0  $\mu\text{M}$  15e in (B) and (F). # $P < 0.05$  versus group of 0  $\mu\text{M}$  15e without HGF and \* $P < 0.05$  versus group of 0  $\mu\text{M}$  15e with HGF in (D).

activity inhibiting Caki-1 cell proliferation ( $\text{IC}_{50} = 0.49 \mu\text{M}$ ) with a 90-fold improvement than that of APG (Table 1). Furthermore, the activity of 15e is 10 times better than that of Crizotinib ( $\text{IC}_{50} = 4.43 \mu\text{M}$ , Table 1), and is also better than the reported  $\text{IC}_{50}$  ( $\text{IC}_{50} = 14.5 \mu\text{M}$  in

Caki-1 cell) for the approved RCC drug Cabozantinib [16]. Therefore, we discovered a new molecular entity 15e with effective anti-RCC activity via structural modification of APG.

Identification of the precise target of APG or its derivative has been a

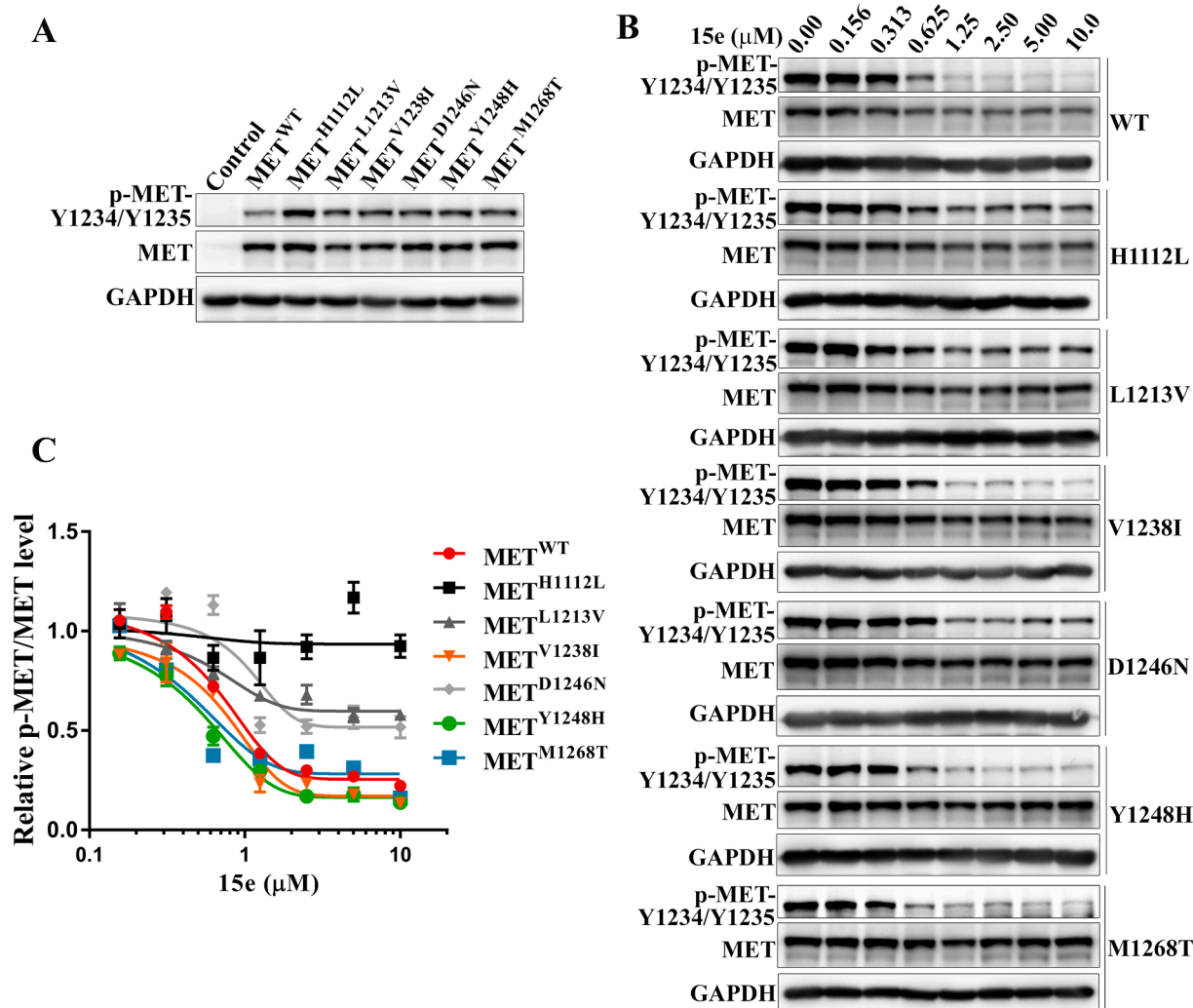


**Fig. 7.** Effects of 15e on phosphorylated activation of mutant MET. (A) MET and p-MET-Y1234/Y1235 in NIH-3 T3 cells transfected with WT or mutant MET plasmid. (B) p-MET-Y1234/Y1235 of WT or mutant MET in NIH-3 T3 cells treated by 0 and 0.156–10  $\mu$ M 15e for 24hrs. (C) Quantification of relative p-MET/MET level of WT or mutant MET under the treatment of 15e concentration gradients. Data are expressed as the mean  $\pm$  SD, n = 3.

challenge. Natural flavonoid APG was discovered several decades ago [48], and many mechanism investigations have been performed. Although APG was demonstrated to affect the expression of many proteins and multiple signal transduction pathways [22], the precise target of APG has not been conclusively identified. A comprehensive study using phage display with high-throughput sequencing found more than 160 APG-binding proteins [23], but also missed some target proteins from other studies [24–26]. The difficulty is partly due to the low potency of APG. Improving the potency is challenging because some of the derivative compounds aggregate at high concentrations and because of their natural fluorescence/color and hence there are arguments whether they were pan-assay interference compounds (PAINS) [49,50]. Now with the more potent APG derivative 15e, we provided a good tool compound to identify the true target for APG. The kinase panel data (Fig. 4) clearly showed that 15e was specifically inhibiting phosphorylation of MET but not other RTKs such as EGFR and RET, and the activity and selectivity were further supported by results shown in Fig. 4 that 15e selectively repressed proliferation of cells with high MET phosphorylation. 15e specifically inhibited RCC in functional experiments *in vitro* and *in vivo* (Fig. 2, 8A). And since MET undergoes auto-phosphorylation, we conclude that MET is the direct target of 15e. Docking modeling of 15e into MET kinase domain fit this hypothesis and the modification at the Ar group indeed make sense (Fig. 5F). These multiple results all supported that 15e is an improved selective MET

inhibitor.

MET has been shown to play critical role in a number of cancers including RCC [4]. Gene amplification and mutations in MET activates downstream pathways and lead to tumor cell proliferation, tumor invasion and pathogenesis [4]. Therefore, if 15e targets MET, it should affect the MET downstream pathways. Our data confirmed that of the three MET classical downstream pathways, PI3K-Akt, Ras-Raf-MEK-Erk and Stat3, 15e mainly affected activation of Akt and Stat3 rather than Erk1/2 in Caki-1 cells stimulated with or without HGF (Fig. 6). Consistent with these data, cells that have high MET and are more dependent on MET for growth are more sensitive to 15e (Fig. 4C–H). Furthermore, with the artificial system where Ba/F3 cells was made to depend on MET, inhibition of TPR-MET kinase activity led to the suppression of cell viability while the activity of 15e was four times less in Ba/F3 cells in the presence of IL-3 (Fig. 5C). Collectively, our data indicate that 15e directly targeted MET, and inhibited MET auto-phosphorylation and its downstream pathways for its anti-RCC activity.

Overcoming MET mutation, especially drug resistant mutation, is important for clinical application. In hereditary and sporadic papillary RCC, MET has been found carrying many constitutively activated mutation such as H112L, L1213V, V1238I, D1246N, Y1248H, or M1268T [9–11], while MET<sup>L1213V/D1246N/Y1248H</sup>, MET<sup>L1213V/D1246N/Y1248H</sup> and MET<sup>V1238I</sup> were resistant to approved MET inhibitor Crizotinib, Capmatinib and Cabozantinib, respectively [12–15]. When tested against

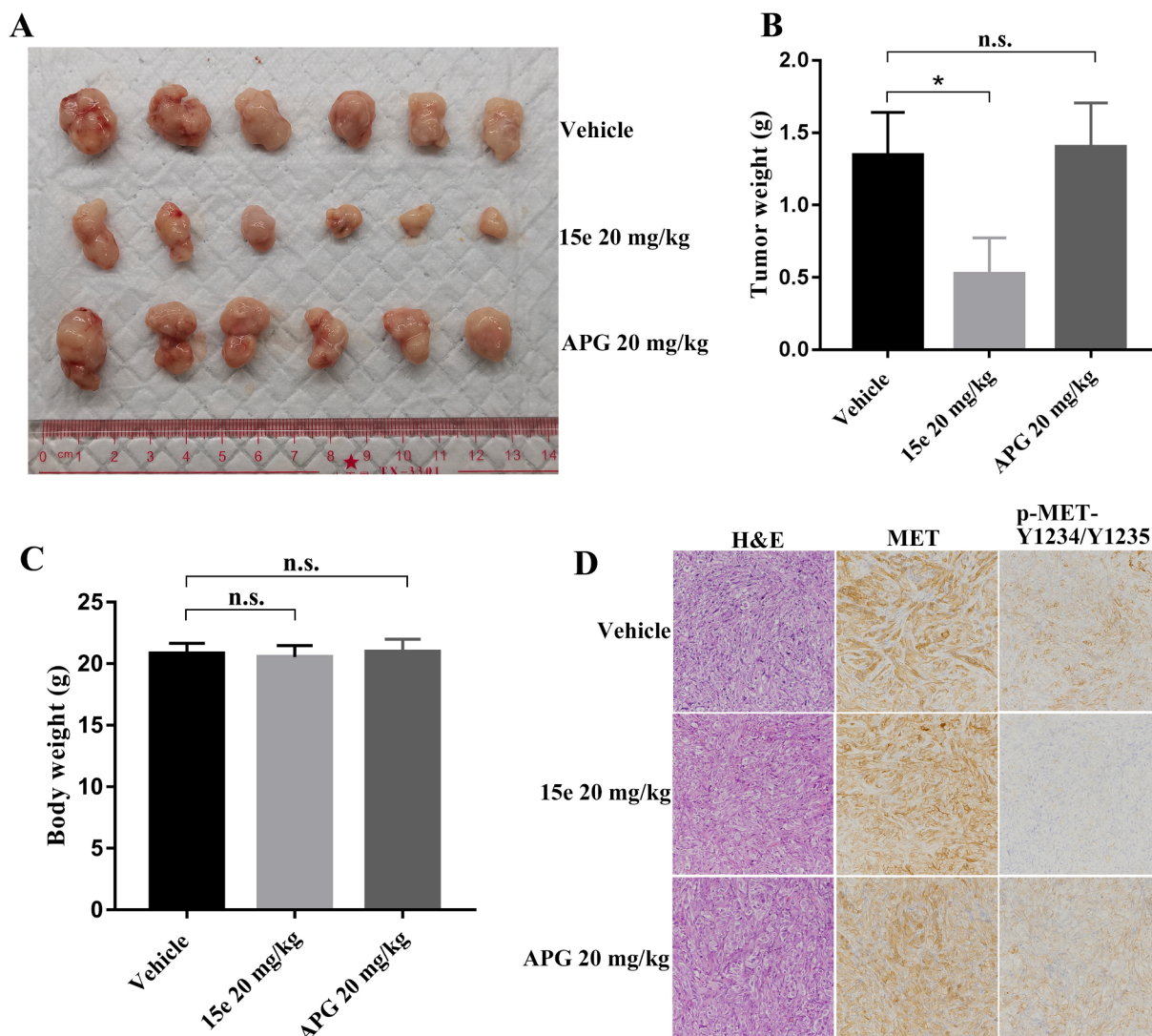


**Fig. 8.** 15e inhibits tumor growth and MET phosphorylation *in vivo*. (A) Photograph of tumors from vehicle, 15e and APG treated mice. (B) Weight of Caki-1 xenograft tumors from nude mice 16 days after treatment. (C) Body weight of mice after treatment. (D) Immunohistochemical staining of Met and p-MET-Y1234/Y1235 in Caki-1 xenograft tumor tissues. Data are expressed as the mean  $\pm$  SD,  $n = 6$ , \* $P < 0.05$  versus Vehicle.

these mutations, 15e was found to still have activity against MET<sup>V1238I</sup>, MET<sup>Y1248H</sup> and MET<sup>M1268T</sup> as well as MET<sup>WT</sup>, while MET<sup>D1246N</sup> and MET<sup>L1213V</sup> were partially inhibited (Fig. 7). Neither of V1238, Y1248 and M1268 in MET kinase domain was key interaction sites of 15e (Fig. 5F), which may explain why 15e still showed activity against MET<sup>V1238I</sup>, MET<sup>Y1248H</sup> and MET<sup>M1268T</sup>. However, D1246, L1213 and especially H1112 were likely important sites for interaction with 15e at MET kinase domain. Collectively, these data are important as 15e could be further developed to treat Crizotinib, Capmatinib or Cabozantinib resistant patients who carry MET<sup>Y1248H</sup> or MET<sup>V1238I</sup> mutations. The activity against the mutant MET implies that the interaction site of 15e with MET is different from previous compounds and indicate that there are potential novel MET inhibitors to be further discovered.

In summary, a series of APG derivatives were synthesized and screened for their anti-RCC activity on Caki-1 cell *in vitro*, and compound 15e was the most potent. 15e was further shown to be able to inhibit cell colony formation, neoplasm growth in 3-D microsphere assay, migration and invasion. Mechanistically, 15e caused cell cycle arrest but not apoptosis. At the molecular level, 15e inhibit auto-phosphorylation of MET at Y1234/Y1235 likely by directly interact with MET kinase domain. As expected, HGF-MET downstream pathways, Akt and Stat3 were downregulated by 15e. Importantly, in addition to MET<sup>WT</sup>, drug

resistant mutant MET<sup>V1238I/Y1248H</sup> can also be abrogated by 15e. *In vivo* study confirmed the inhibitive activity of 15e in RCC growth and MET phosphorylation. These results indicate 15e is a promising novel candidate for RCC therapy, and especially provide a potential alternative to overcome drug-resistant MET<sup>V1238I/Y1248H</sup> in RCC.

#### CRediT authorship contribution statement

**Jing Li:** Conceptualization, Methodology, Validation, Formal analysis, Investigation, Writing - original draft, Project administration. **Guishan Tan:** Supervision, Funding acquisition. **Yabo Cai:** Conceptualization, Methodology, Validation, Formal analysis, Investigation, Writing - original draft. **Ruihuan Liu:** Supervision. **Xiaolin Xiong:** Investigation. **Baohua Gu:** Validation, Formal analysis, Writing - original draft. **Wei He:** Investigation. **Bing Liu:** . **Qingyun Ren:** Conceptualization. **Jianping Wu:** Validation. **Bo Chi:** Writing - original draft. **Hang Zhang:** Writing - original draft. **Yanzhong Zhao:** Validation, Formal analysis. **Yangrui Xu:** Investigation. **Zhenxing Zou:** Validation, Formal analysis. **Fenghua Kang:** Validation, Formal analysis. **Kangping Xu:** Conceptualization, Supervision, Funding acquisition.

## Declaration of Competing Interest

The authors declare that they have no known competing financial interests or personal relationships that could have appeared to influence the work reported in this paper.

## Acknowledgements

This work was supported by the Construction Program of Hunan's innovative Province (CN) - High-tech Industry Science and Technology Innovation Leading Project (2020SK2002), Central South University postgraduate independent exploration and innovation project (No. 2018zzts239, No. 2020zzts821), Key Project of Changsha Science and Technology Plan (No. kq1801072), National Natural Science Foundation of China (31370370), Central South University Deepening Innovation and Entrepreneurship Education Reform Research Project (No. 2019CG006), Hunan Province Ordinary Higher Education Teaching Reform Research Project, Open Sharing Fund for the Large-scale Instruments and Equipments of Central South University. We are very grateful to Prof. Guogen Liu (Modern Analysis and Testing Centre of Central South University) for the NMR tests. We thank Dr. Jiuzhong Huang and Dr. Chuanfei Jin at Sunshine Lake Pharma Co., Ltd for suggestions on compound synthesis. We thank Dr. Ming Li at Shanghai Institute of Materia Medica Chinese Academy of Science for Caki-2 and ACHN cell assay.

## References

- J.J. Hsieh, M.P. Purdue, S. Signoretti, C. Swanton, L. Albiges, M. Schmidinger, D. Y. Heng, J. Larkin, V. Ficarra, Renal cell carcinoma, *Nat. Rev. Dis. Primers* 3 (1) (2017), <https://doi.org/10.1038/nrdp.2017.9>.
- Cancer Genome Atlas Research N Comprehensive molecular characterization of clear cell renal cell carcinoma, *Nature*, 2013; 499: 43-49.
- Cancer Genome Atlas Research N, Linehan WM, Spellman PT, Ricketts CJ, Creighton CJ, Fei SS, et al. Comprehensive Molecular Characterization of Papillary Renal-Cell Carcinoma, *N Engl J Med*, 2016; 374: 135-145.
- R.R. Kotecha, R.J. Motzer, M.H. Voss, owards individualized therapy for metastatic renal cell carcinoma, *Nat. Rev. Clin. Oncol.* 16 (10) (2019) 621-633.
- A. Giubellino, W.M. Linehan, D.P. Bottaro, Targeting the Met signaling pathway in renal cancer, *Expert Rev. Anticancer Ther.* 9 (6) (2009) 785-793.
- G. Recondo, J. Che, P.A. Jänne, M.M. Awad, Targeting MET dysregulation in cancer, *Cancer Discov.* 10 (7) (2020) 922-934.
- P. Longati, A. Bardelli, C. Ponzetto, L. Naldini, P.M. Comoglio, Tyrosines1234-1235 are critical for activation of the tyrosine kinase encoded by the MET proto-oncogene (HGF receptor), *Oncogene* 9 (1994) 49-57.
- E. Gherardi, W. Birchmeier, C. Birchmeier, G.V. Woude, Woude G. Vande, Targeting MET in cancer: rationale and progress, *Nat. Rev. Cancer* 12 (2) (2012) 89-103.
- L. Schmidt, F.-M. Duh, F. Chen, T. Kishida, G. Glenn, P. Choyke, S.W. Scherer, Z. Zhuang, I. Lubensky, M. Dean, R. Allikmets, A. Chidambaram, U.R. Bergerheim, J.T. Feltis, C. Casadevall, A. Zamarron, M. Bernues, S. Richard, C.J.M. Lips, M. M. Walther, L.-C. Tsui, L. Geil, M.L. Orcutt, T. Stackhouse, J. Lipan, L. Slife, H. Brauch, J. Decker, G. Niehans, M.D. Hughson, H. Moch, S. Storkel, M.I. Lerman, W.M. Linehan, B. Zbar, Germline and somatic mutations in the tyrosine kinase domain of the MET proto-oncogene in papillary renal carcinomas, *Nat. Genet.* 16 (1) (1997) 68-73.
- E.A. Tovar, C.R. Graveel, MET in human cancer: germline and somatic mutations, *Ann. Transl. Med.* 5 (2017) 205.
- M. Jeffers, L. Schmidt, N. Nakaigawa, C.P. Webb, G. Weirich, T. Kishida, B. Zbar, G. F. Vande Woude, Activating mutations for the met tyrosine kinase receptor in human cancer, *Proc. Natl. Acad. Sci. U.S.A.* 94 (21) (1997) 11445-11450.
- T. Fujino, Y. Kobayashi, K. Suda, T. Koga, M. Nishino, S. Ohara, et al., Sensitivity and Resistance of MET Exon 14 Mutations in Lung Cancer to Eight MET tyrosine kinase inhibitors in vitro, *J. Thorac. Oncol.* 14 (2019) 1753-1765.
- S. Baltschukat, B.S. Engstler, A. Huang, H.-X. Hao, A. Tam, H.Q. Wang, J. Liang, M. T. DiMare, H.-E. Bhang, Y. Wang, P. Furet, W.R. Sellers, F. Hofmann, J. Schoepfer, R. Tiedt, Capmatinib (INC280) is active against models of non-small cell lung cancer and other cancer types with defined mechanisms of MET activation, *Clin. Cancer Res.* 25 (10) (2019) 3164-3175.
- L.D. Engstrom, R. Aranda, M. Lee, E.A. Tovar, C.J. Essenburg, Z. Madaj, H. Chiang, D. Briere, J. Hallin, P.P. Lopez-Casas, N. Baños, C. Menendez, M. Hidalgo, V. Tassell, R. Chao, D.I. Chudova, R.B. Lanman, P. Olson, L. Bazhenova, S.P. Patel, C. Graveel, M. Nishino, G.I. Shapiro, N. Peled, M.M. Awad, P.A. Jänne, J. G. Christensen, Glesatinib exhibits antitumor activity in lung cancer models and patients harboring MET Exon 14 mutations and overcomes mutation-mediated resistance to type I MET inhibitors in nonclinical models, *Clin. Cancer Res.* 23 (21) (2017) 6661-6672.
- J. Song, Y. Kwon, S. Kim, S.K. Lee, Antitumor activity of phenanthroindolizidine alkaloids is associated with negative regulation of Met endosomal signaling in renal cancer cells, *Chem. Biol.* 22 (4) (2015) 504-515.
- M. Miller, K. Ginalski, B. Lesyng, N. Nakaigawa, L. Schmidt, B. Zbar, B. Zbar, Structural basis of oncogenic activation caused by point mutations in the kinase domain of the MET proto-oncogene: modeling studies, *Proteins* 44 (1) (2001) 32-43.
- N. Nakaigawa, M. Yao, M. Baba, S. Kato, T. Kishida, K. Hattori, Y. Nagashima, Y. Kubota, Inactivation of von Hippel-Lindau gene induces constitutive phosphorylation of MET protein in clear cell renal carcinoma, *Cancer Res.* 66 (7) (2006) 3699-3705.
- S. Pennacchietti, P. Michieli, M. Galluzzi, M. Mazzone, S. Giordano, P. M. Comoglio, Hypoxia promotes invasive growth by transcriptional activation of the met protooncogene, *Cancer Cell* 3 (4) (2003) 347-361.
- R.R. Oh, J.Y. Park, J.H. Lee, M.S. Shin, H.S. Kim, S.K. Lee, Y.S. Kim, S.H. Lee, S. N. Lee, Y.M. Yang, N.J. Yoo, J.Y. Lee, W.S. Park, Expression of HGF/SF and Met protein is associated with genetic alterations of VHL gene in primary renal cell carcinomas, *APMIS* 110 (3) (2002) 229-238.
- G.T. Gibney, S.A. Aziz, R.L. Camp, P. Conrad, B.E. Schwartz, C.R. Chen, W.K. Kelly, H.M. Kluger, c-Met is a prognostic marker and potential therapeutic target in clear cell renal cell carcinoma, *Ann. Oncol.* 24 (2) (2013) 343-349.
- Y. Miyata, H. Kanetake, S. Kanda, Presence of phosphorylated hepatocyte growth factor receptor/c-Met is associated with tumor progression and survival in patients with conventional renal cell carcinoma, *Clin. Cancer Res.* 12 (16) (2006) 4876-4881.
- J. Madunić, I.V. Madunić, G. Gajski, J. Pocić, V. Garaj-Vrhovac, Apigenin: A dietary flavonoid with diverse anticancer properties, *Cancer Lett.* 413 (2018) 11-22.
- D. Arango, K. Morohashi, A. Yilmaz, K. Kuramochi, A. Parihar, B. Brahimaj, E. Grotewold, A.I. Doseff, Molecular basis for the action of a dietary flavonoid revealed by the comprehensive identification of apigenin human targets, *Proc. Natl. Acad. Sci. U.S.A.* 110 (24) (2013) E2153-E2162.
- S. Byun, J. Park, E. Lee, S. Lim, J.G. Yu, S.J. Lee, et al., Src kinase is a direct target of apigenin against UVB-induced skin inflammation, *Carcinogenesis* 34 (2013) 397-405.
- C.A. Franzen, E. Amargo, V. Todorović, B.V. Desai, S. Huda, S. Mirzoeva, K. Chiu, B.A. Grzybowski, T.-L. Chew, K.J. Green, J.C. Pelling, The chemopreventive bioflavonoid apigenin inhibits prostate cancer cell motility through the focal adhesion kinase/Src signaling mechanism, *Cancer Prev. Res. (Phila)* 2 (9) (2009) 830-841.
- S. Lamy, V. Bedard, D. Labbe, H. Sartelet, C. Barthomeuf, D. Gingras, et al., The dietary flavones apigenin and luteolin impair smooth muscle cell migration and VEGF expression through inhibition of PDGFR-beta phosphorylation, *Cancer Prev. Res. (Phila)* 1 (2008) 452-459.
- R. Liu, H. Zhang, M. Yuan, J. Zhou, Q. Tu, J.-J. Liu, J. Wang, Synthesis and biological evaluation of apigenin derivatives as antibacterial and antiproliferative agents, *Molecules* 18 (9) (2013) 11496-11511.
- X. Zheng, L. Yu, J. Yang, X. Yao, W. Yan, S. Bo, et al., Synthesis and anti-cancer activities of apigenin derivatives, *Med. Chem.* 10 (2014) 747-752.
- B. Kim, N. Jung, S. Lee, J.K. Sohng, H.J. Jung, Apigenin Inhibits Cancer Stem Cell-Like Phenotypes in Human Glioblastoma Cells via Suppression of c-Met Signaling, *Phytother. Res.* 30 (11) (2016) 1833-1840.
- H.E. Elsayed, H.Y. Ebrahim, M.M. Mohyeldin, A.B. Siddique, A.M. Kamal, E. G. Haggag, K.A. El Sayed, Rutin as A novel c-met inhibitory lead for the control of triple negative breast malignancies, *Nutr. Cancer* 69 (8) (2017) 1256-1271.
- G.-S. Xia, S.-H. Li, W. Zhou, Isoquercitrin, ingredients in Tetrastrigma hemsleyanum Diels et Gilg, inhibits hepatocyte growth factor/scatter factor-induced tumor cell migration and invasion, *Cell Adh. Migr.* (2018) 464-471.
- M.-D. Shi, Y.-C. Liao, Y.-W. Shih, L.-Y. Tsai, Nobiletin attenuates metastasis via both ERK and PI3K/Akt pathways in HGF-treated liver cancer HepG2 cells, *Phytomedicine* 20 (8-9) (2013) 743-752.
- W.J. Lee, W.K. Chen, C.J. Wang, W.L. Lin, T.H. Tseng, Apigenin inhibits HGF-promoted invasive growth and metastasis involving blocking PI3K/Akt pathway and beta 4 integrin function in MDA-MB-231 breast cancer cells, *Toxicol. Appl. Pharmacol.* 226 (2008) 178-191.
- S. Meng, Y.i. Zhu, J.-F. Li, X. Wang, Z. Liang, S.-Q. Li, X. Xu, H. Chen, B. Liu, X.-Y. Zheng, L.-P. Xie, Apigenin inhibits renal cell carcinoma cell proliferation, *Oncotarget* 8 (12) (2017) 19834-19842.
- W. Deng, W. Han, T. Fan, X. Wang, Z. Cheng, B.o. Wan, J. Chen, Scutellarin inhibits human renal cancer cell proliferation and migration via upregulation of PTEN, *Biomed. Pharmacother.* 107 (2018) 1505-1513.
- Y. Li, Q. Sun, H. Li, B. Yang, M. Wang, Vitexin suppresses renal cell carcinoma by regulating mTOR pathways, *Transl. Androl. Urol.* 9 (4) (2020) 1700-1711.
- G. Pan, Y. Ma, K.e. Yang, X. Zhao, H. Yang, Q. Yao, K. Lu, T. Zhu, P. Yu, Total synthesis of (-)-Anastatin A and B, *Tetrahedron Lett.* 56 (30) (2015) 4472-4475.
- D. Muller, J.-P. Fleury, A new strategy for the synthesis of biflavonoids via arylboronic acids, *Tetrahedron Lett.* 32 (20) (1991) 2229-2232.
- G. Sagraera, G. Seoane, Total synthesis of 3',3''-Binaringenin and related biflavonoids, *Synthesis* 2010 (16) (2010) 2776-2786.
- Y. Kimura, K.-I. Oyama, T. Kondo, K. Yoshida, Synthesis of 8-aryl-3,5,7,3',4'-penta-O-methylcyanidins from the corresponding quercetin derivatives by reduction with LiAlH<sub>4</sub>, *Tetrahedron Lett.* 58 (10) (2017) 919-922.
- F. Yin, A.E. Giuliano, A.J. Van Herle, Signal pathways involved in apigenin inhibition of growth and induction of apoptosis of human anaplastic thyroid cancer cells (ARO), *Anticancer Res.* 19 (1999) 4297-4303.

- [42] M. Warmuth, S. Kim, X.J. Gu, G. Xia, F. Adrian, Ba/F3 cells and their use in kinase drug discovery, *Curr. Opin. Oncol.* 19 (2007) 55–60.
- [43] P.C. Ma, E. Schaefer, J.G. Christensen, R. Salgia, A selective small molecule c-MET Inhibitor, PHA665752, cooperates with rapamycin, *Clin. Cancer Res.* 11 (6) (2005) 2312–2319.
- [44] C.S. Cooper, M. Park, D.G. Blair, M.A. Tainsky, K. Huebner, C.M. Croce, G.F. Vande Woude, Molecular cloning of a new transforming gene from a chemically transformed human cell line, *Nature* 311 (5981) (1984) 29–33.
- [45] J. Porter, S. Lumb, F. Lecomte, J. Reuberson, A. Foley, M. Calmiano, K. le Riche, H. Edwards, J. Delgado, R.J. Franklin, J.M. Gascon-Simorte, A. Maloney, C. Meier, M. Batchelor, Discovery of a novel series of quinoxalines as inhibitors of c-Met kinase, *Bioorg. Med. Chem. Lett.* 19 (2) (2009) 397–400.
- [46] B.D. Manning, A. Toker, AKT/PKB signaling: navigating the network, *Cell* 169 (3) (2017) 381–405.
- [47] R.J. Motzer, T.E. Hutson, L. McCann, K. Deen, T.K. Choueiri, Overall survival in renal-cell carcinoma with pazopanib versus sunitinib, *N. Engl. J. Med.* 370 (18) (2014) 1769–1770.
- [48] D.F. Birt, B. Walker, M.G. Tibbels, E. Bresnick, Anti-mutagenesis and anti-promotion by apigenin, robinetin and indole-3-carbinol, *Carcinogenesis* 7 (6) (1986) 959–963.
- [49] J. Glaser, U. Holzgrabe, Focus on PAINS: false friends in the quest for selective anti-protozoal lead structures from Nature? *MedChemComm* 7 (2) (2016) 214–223.
- [50] J. Bisson, J.B. McAlpine, J.B. Friesen, S.-N. Chen, J. Graham, G.F. Pauli, Can invalid bioactives undermine natural product-based drug discovery? *J. Med. Chem.* 59 (5) (2016) 1671–1690.